



THERMOLUMINESCENCE PROPERTIES OF DY DOPED LIMGPO₄ PHOSPHOR

S.P. Puppalwar^{a*}, S.J. Dhoble^b, P.W. Yawalkar^c

^aDepartment of Physics, Kamla Nehru Mahavidyalaya, Nagpur 440024, India

^bDepartment of Physics, R.T.M. Nagpur University, Nagpur 440033, India

^cDepartment of Physics, Nabira Mahavidyalaya, Katol, India

ABSTRACT

LiMgPO₄:Dy phosphor was prepared by modified solid state reaction technique. The crystalline phase, size, fluorescence and dosimetric properties were characterized by X-ray diffraction (XRD), photoluminescence (PL) and thermoluminescence (TL) spectra, respectively. LiMgPO₄:Dy exhibits a main TL peak at 160°C with a hump at 232°C. The prepared phosphor showed very less fading and the intensity of glow peak at 160°C was observed 1.64 times more than commercially TLD material (CaSO₄:Dy). In the photoluminescence emission spectra, the LiMgPO₄:Dy³⁺ show efficient blue (483 nm) and yellow (576 nm) bands when excited by 350 nm. TL and PL studies exhibit Dy³⁺ ion as the luminescence centre in this phosphor. The activation energy and frequency factor obtained are 1.076 eV and $1.16 \times 10^{12} \text{ s}^{-1}$, respectively. The results show the glow curve peak of LiMgPO₄:Dy³⁺ obey first order kinetics. The dosimetric characteristics like dose response, fading, and kinetic parameters, namely activation energy (E) and frequency factor (s) associated with the main glow peak are discussed in this paper.

Keywords: LiMgPO₄, Photoluminescence, Thermoluminescence, Kinetic Parameters, Peak shape method

1. Introduction

Thermoluminescence dosimetry (TLD) has been widely applied in areas such as clinical, personal and environmental monitoring of ionizing radiation. High sensitivity, tissue equivalent, thermoluminescence dosimetry (TLD) materials with simple glow curves and

good thermal stability are important for the measurement of exposures in the field of medical physics. There are a number of commercially available thermoluminescent dosimeters (TLD) for this purpose under different trade names. But, efforts are still being made by either improve the TL characteristics of these materials by synthesizing them using different methods or by doping with different impurities [1–3] or developing some new ones [4–6]. These phosphors can be used either in the personal or environmental radiation dosimetry. Phosphates are the promising host materials for their chemical/thermal stabilities over a wide range of temperatures [7]. Phosphates of general formula ABPO₄, where A is a monovalent and B is a divalent cation, are of interest for their optical [8] properties. Though ABPO₄ materials were found to be efficient hosts [9, 10], luminescence studies in LiMgPO₄ are few. Dhabekar et al. have synthesized LiMgPO₄ based phosphor with Tb and B as dopants and observed it to be a sensitive OSL phosphor [11].

During our investigation in Li based compounds we have found there is no work on Dy doped LiMgPO₄ which having interesting TL properties that could be used for dosimetric applications. The dosimetric characteristic of any TL phosphor mainly depends on its trapping parameters such as the traps depth E, frequency factor s and order of kinetics b [12, 13], which describe the defect centers responsible for the TL emission in material. In this study, we have reported photoluminescence (PL), thermoluminescence (TL) properties and kinetic parameters of LiMgPO₄:Dy phosphor. The order of kinetics (b), activation energy (E)

and frequency factor (s) were determined by peak shape (PS) method.

2. Experimental

$\text{LiMgPO}_4\text{:Dy}$ was prepared by the high temperature solid state reaction method. Li_2CO_3 , MgCO_3 , $\text{NH}_4\text{H}_2\text{PO}_4$ and Dy_2O_3 all analytical grades were taken as starting materials in stoichiometric ratio. The stoichiometric amounts of starting materials were weighted and thoroughly mixed in an agate mortar for half an hour, then transferred to the silica crucible. The samples were first preheated at 550 °C in air for the sufficient diffuse and infiltration of the starting materials, with a soaking time of 3h, for which the samples were firing. Secondly, the preheated mixtures were milled sufficiently again after cooling and then fired at 950 °C for 10 h in air to obtain the final products.

The XRD technique was used in order to identify the product and check their crystallinity. The phase composition and phase structure were characterized by X-ray diffraction (XRD) pattern using a PAN-analytical diffractometer with Cu K α radiation ($\lambda=1.5405 \text{ \AA}$) operating at 40Kv, 30mA. The XRD data were collected in a 2θ range from 10 to 80°, with the continuous scan mode. The morphology and microstructure were characterized with JEOL, JSM-6360LV SEM environmental scanning electron microscope (SEM). For the TL measurement samples were exposed to gamma rays from ^{60}Co at room temperature. After the desired exposure, TL glow curves were recorded for 5 mg of sample each time at a heating rate of 5 °C/s. TL glow curves were recorded with the usual set up Nucleonix TL – 1009. For comparison, glow curves were also recorded under identical conditions for commercially available dosimetry grade TLD - $\text{CaSO}_4\text{:Dy}$. The photoluminescence excitation and emission

spectra were measured at room temperature by using a RF-5301PC SHIMADZU Spectrofluorophotometer equipped with a 150W Xenon lamp as the excitation source.

3. Results & Discussion

3.1. X-ray diffraction and morphology

Rare earth element orthophosphates display a variety of structures. They appear in hexagonal, tetragonal and monoclinic modifications. The structure of $\text{LiMgPO}_4\text{:Dy}$ prepared by high temperature solid state reaction method in our work is hexagonal. Fig. 1 shows the XRD pattern of LiMgPO_4 phosphor along with the standard XRD pattern (JCPDS card no. 32-0574). The XRD pattern shows the formation of pure LiMgPO_4 phase. The addition of the dopant has no effect on the XRD pattern. All the peaks are due to LiMgPO_4 single phase and no impurity peaks were observed. However, some new diffraction peaks also emerge, which are characteristic diffraction peaks for the prepared samples, but cannot be attributed to any known compounds. The slow scan was performed in the 2θ range from 10–80°. Based on the effective ionic radius of cations with different coordination numbers, it is assumed that Dy^{3+} ions are preferably to replace Mg^{2+} ions. The shape and size of the prepared crystalline powder LiMgPO_4 were determined by scanning electron microscope (SEM) using JEOL; JSM-6360LV SEM. SEM images are shown in Fig. 2. The particles of different shapes and sizes could be seen in this photograph. It shows hexagonal structure-like particles. Although a small amount of particles can be observed occasionally, the interweaving particles are very neat and straight with an average diameter around 400 nm and lengths ranging from 2 to 3 μm . This non-uniform particle size is caused due to the non-uniform distribution of temperature and mass flow during the synthesis.

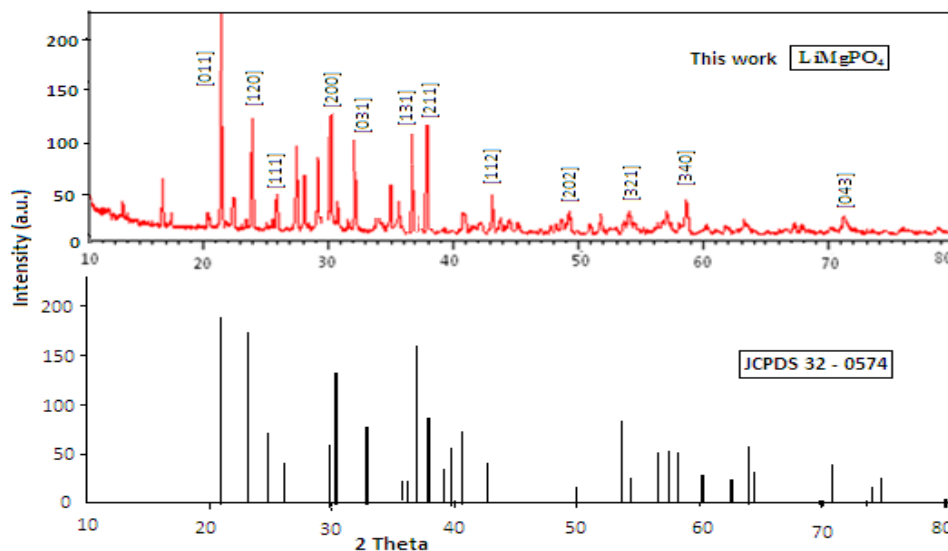


Fig. 1. X- ray diffraction pattern of LiMgPO₄ alongwith JCPDS card 32-0574.

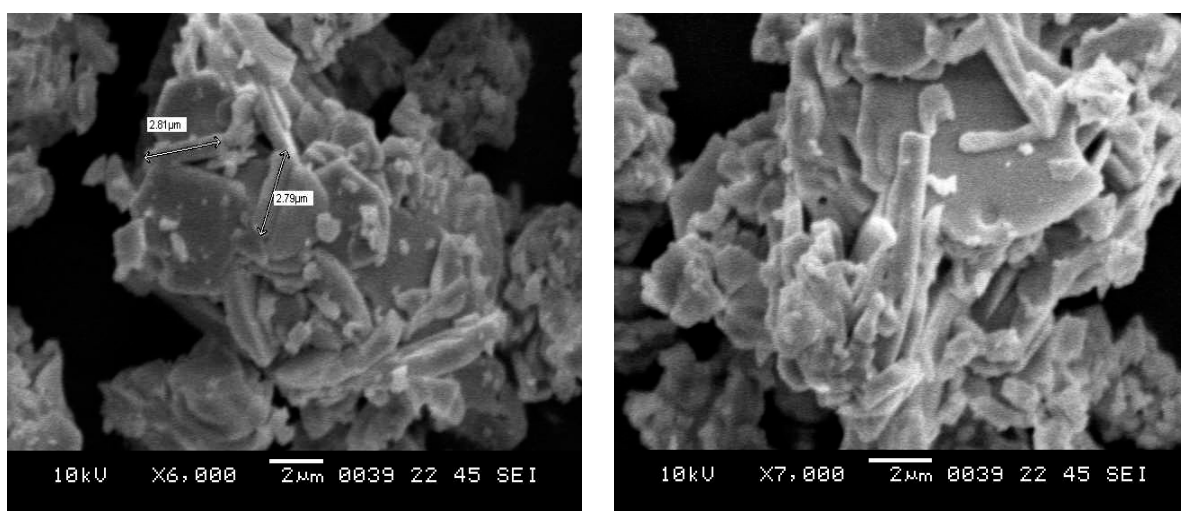


Fig.2 SEM images of LiMgPO₄

3.2 Photoluminescence

To analyze the luminescence properties as a function of Dy³⁺ ion concentration, the excitation spectrum was recorded in the spectral region 300 – 400 nm for the LiMgPO₄:Dy³⁺ by monitoring the emission at 483 nm, as shown in Fig. 3. The excitation peaks at 350, 362 and 386 nm have been assigned to the transitions from ⁶H_{15/2} to ⁴I_{15/2} and ⁴F_{9/2} of Dy³⁺. The excitation band centered at 350 nm (⁶H_{15/2} → ⁶P_{7/2}) is found to be more intense. In the photoluminescence emission spectra, the LiMgPO₄:Dy³⁺ phosphors show efficient blue (483 nm) and yellow (576 nm) bands at the excitation of 350 nm wavelength of UV light. The emission spectra for the Dy³⁺ doped samples are composed of the characteristic emission lines of Dy³⁺ with ⁴f₉ configuration. The blue emission band is typical emission of Dy³⁺ ion assigned to ⁴F_{9/2} → ⁶H_{15/2} transition and yellow emission is assigned to ⁴F_{9/2}

→ ⁶H_{13/2} transition. The ⁴F_{9/2} - ⁶H_{13/2} transition is a hypersensitive electronic dipole transition ($\Delta J = \pm 2$) which has been strongly influenced by the coordination environment. On the other hand, the ⁴F_{9/2} - ⁶H_{15/2} transition is a magnetic dipole transition ($\Delta J = 0, \pm 1$ but 0 – 0 forbidden) and less sensitive to the coordination environment [14]. Thus the yellow-to-blue luminescence intensity ratio (Y/B) has been used to characterize the Dy³⁺ – O²⁻ bond covalence and the higher value of Y/B indicates the higher degree of co-valences between Dy³⁺ and O²⁻ ions [15]. Thus, the yellow and blue ratio known as the asymmetry ratio of Dy³⁺ ion varies while locating in different host lattices. The optical properties of the material are often influenced by the structure of the matrix and synthesis technique. It is found that the intensity of Dy³⁺ increases with increase of the concentration of Dy³⁺ ion, reaching a maximum value at 2 mol% of Dy³⁺ with no clue of

saturation up to the higher concentration in the host lattice.

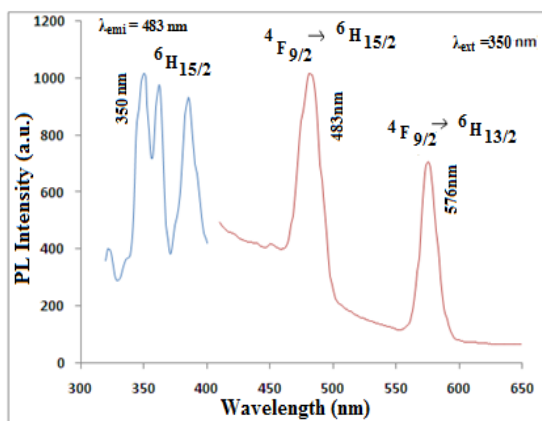


Fig. 3. PL excitation ($\lambda_{\text{emi}} = 483 \text{ nm}$) and emission ($\lambda_{\text{ext}} = 350 \text{ nm}$) spectra of $\text{LiMgPO}_4:0.02\text{Dy}^{3+}$ phosphor.

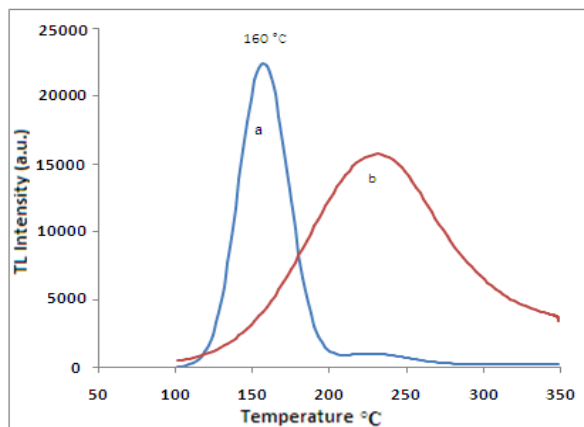


Fig. 4. TL glow curve of (a) $\text{LiMgPO}_4:0.02\text{Dy}^{3+}$ and (b) TLD $\text{CaSO}_4:\text{Dy}$ for 3Gy γ -ray irradiation at room temperature.

3.3 Thermoluminescence

TL properties of $\text{LiMgPO}_4:\text{Dy}$ samples were first time studied in detail. The TL glow curves have been recorded at a heating rate of 5°C/s and irradiation at a dose rate of 0.42kGy/h at room temperature. TL glow curves of $\text{LiMgPO}_4:0.02\text{Dy}$ exposed to 3 Gy of ^{60}Co γ -rays, together with the glow curve of the commercially available dosimeter $\text{CaSO}_4:\text{Dy}$ are shown in Fig. 4. The glow curves consist of a prominent TL peak located at 160°C and a hump around 232°C . The intensities of the

glow peaks were found to increase with the increase of concentration of Dy^{3+} . The TL intensity is optimum for 2 mole% of concentration of Dy^{3+} ion. The shape and position of the TL glow peak keep almost constant in the concentration range. TL glow curves of $\text{LiMgPO}_4:\text{Dy}$ with different Dy^{3+} concentrations irradiated with a 3 Gy γ -ray dose at room temperature are shown in Fig. 5. It is also observed that the TL intensity of reported phosphor is 1.64 times more than that of $\text{CaSO}_4:\text{Dy}$.

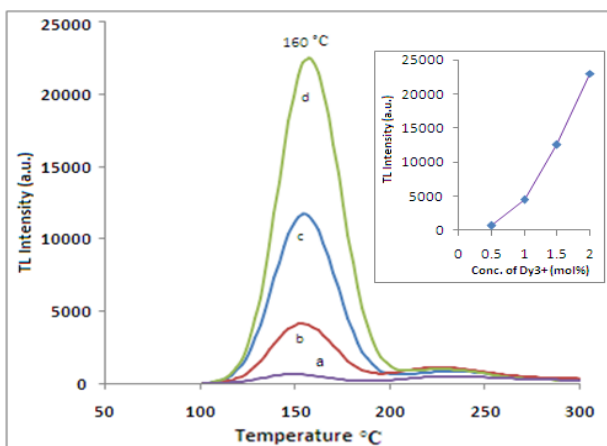


Fig. 5. TL glow curves of $\text{LiMgPO}_4:\text{Dy}$ with different Dy^{3+} concentrations irradiated by γ -ray dose of 3Gy. The mole fraction of Dy^{3+} ion was (a) 0.5 mol%, (b) 1 mol%, (c) 1.5 mol%, and (d) 2 mol%. The inset shows dependence of TL response of high temperature peak on Dy^{3+} concentration.

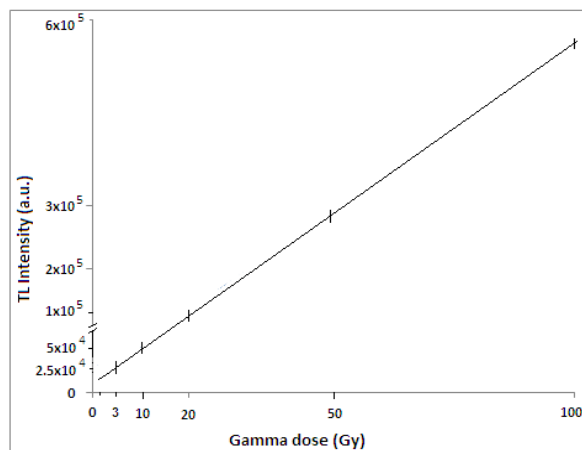


Fig. 6. Linearity range of the TL responses of the $\text{LiMgPO}_4:0.02\text{Dy}^{3+}$ phosphor vs absorbed doses.

An important property of a TL dosimeter material is that it exhibits a linear relation between TL intensity and absorbed dose. The intensity of the 160°C peak is plotted as a function of the dose in Fig. 6. It is seen that the response curve of $\text{LiMgPO}_4:\text{Dy}$ (2 mol %) is linear up to a dose of 100Gy. This result shows that the phosphor can be used for high dose

dosimetry like food irradiation dosimetry. TL intensity increases as dose increases, with no clue of saturation up to the higher investigated dose. Stability of the whole glow curve leads to negligible changes in the integrated TL. Therefore it could be expected that its application is suitable for low dose in radiation protection dosimetry as well as high dose

dosimetry like food irradiation dosimetry. The post-irradiation storage stability of TL signal in $\text{LiMgPO}_4:\text{Dy}^{3+}$ powder at room temperature with storage time is given in Fig.7. It shows a very small decrease of the TL response during the

elapsed period of time in the dosimetric peak of the samples. The fading of this peak is less than 10% for 10 days if the dosimeters were protected from direct room light.

3.4 Dosimetric characteristics

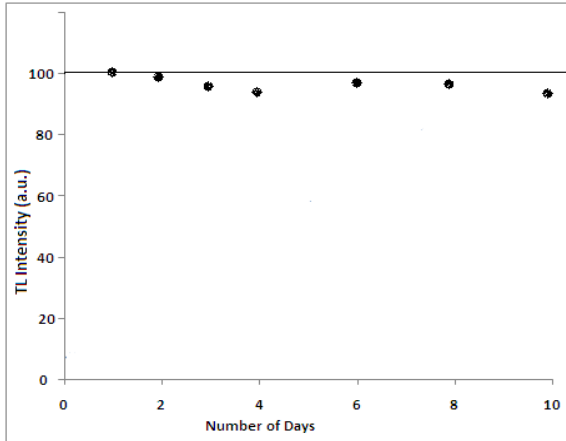


Fig. 7. Post-irradiation TL fading in the γ -irradiated $\text{LiMgPO}_4:0.02\text{Dy}$ powder sample for the duration of 10 days storage in room temperature; irradiation dose — 3 Gy.

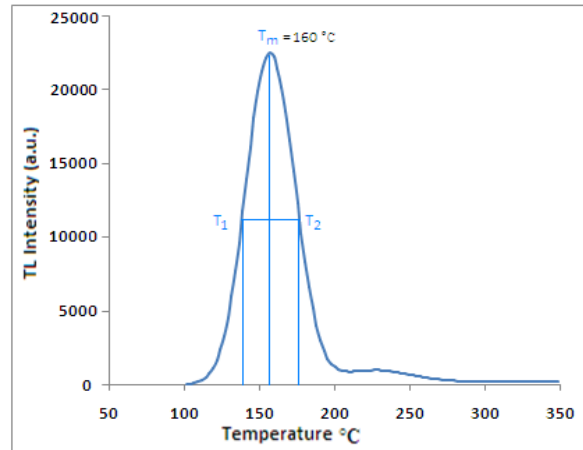


Fig.8. TL glow curve of (a) $\text{LiMgPO}_4:0.02\text{Dy}^{3+}$ for 3Gy dose of γ - rays.

The kinetic parameters of the main TSL peak were determined using peak shape method [16]. This method is valid for any order of kinetics. This method is mainly based on the temperatures T_m , T_1 and T_2 , where T_m is the peak temperature, while T_1 and T_2 are temperatures at half the intensity on the ascending and descending parts of the glow peak respectively. To determine the kinetic parameters the following shape parameters are to be determined: the total half intensity width $\omega = T_2 - T_1$, the high temperature half width $\delta = T_2 - T_m$ and the low temperature half width $\tau = T_m - T_1$ [17]. The peak shape method is mainly used to calculate the order of kinetics.

Order of kinetics can be evaluated from the symmetry factor (μ_g) of the glow peak. μ_g is calculated using Eq. (1) from the known peak shape parameters δ and ω . Order of the kinetics depends on the glow peak shape. The value of μ_g for first and second order kinetics is 0.42 and 0.52 respectively. Chen has provided a plot which gives order of kinetics of the TL process, according to the value of the geometric factor (μ_g).

$$(\mu_g) = \delta / \omega = T_2 - T_m / T_2 - T_1 \quad \text{----- (1)}$$

In Fig 8, T_1 , T_m and T_2 are 139°C (412K), 160°C (433K) and 176°C (449K), respectively. Inserting these values in Eq. (1), symmetry factor (μ_g) is obtained about 0.43 suggests that this peak obeys first-order kinetics. Furthermore

Furetta et al. [18] has proposed the following parameter:

$$\gamma = \delta / \tau = T_2 - T_m / T_m - T_1 \quad \text{----- (2)}$$

This parameter ranges from 0.7 to 0.8 for first-order kinetics and from 1.05 to 1.20 for second-order kinetics. This parameter (γ) for the 160 °C glow peak of $\text{LiMgPO}_4:\text{Dy}$ was found to be 0.76, which suggests that this peak obeys first-order kinetics. Generally in the first order, the process of retrapping is negligible and the trap should be situated very close to the luminescent centre. For a fixed heating rate, in first order kinetics both peak temperature and shape are independent of the initial trapped electron concentration but in second order the peak temperature and shape are strongly dependent on initial trapped charge concentration. The activation energy (E) can be calculated by the general expressions formulated by Chen, valid for any kinetics, and is given by:

$$E = c_\alpha (kT_m^2 / \alpha) - b_\alpha (2kT_m) \quad \text{----- (3)}$$

where α stands for τ , δ and ω respectively. c_α and b_α are obtained using the expressions given below:

$$c_\tau = 1.51 + 3.0(\mu_g - 0.42),$$

$$b_\tau = 1.58 + 0.42(\mu_g - 0.42)$$

$$c_\delta = 0.976 + 7.3(\mu_g - 0.42), \quad b_\delta = 0$$

$$c_\omega = 2.52 + 10.2(\mu_g - 0.42), \quad b_\omega = 1,$$

The activation energies for the 160 °C glow peak of $\text{LiMgPO}_4:\text{Dy}$ when calculated by Eq. (3) using low-temperature half width, high

temperature half width and full width of the peak at its half height were found to be 1.08, 1.07 and 1.08 eV giving mean value of activation energy 1.076 eV. Once orders of kinetics and activation energy were determined, the frequency factor (s) was calculated [19] by the equation given bellow:

$$\beta E / kT_m^2 = s [1 + (b-1) 2kT_m / E] \exp (-E / kT_m) \quad \text{----- (4)}$$

where 'b' is order of kinetics and 'β' is the heating rate. The frequency factor for the 168 °C glow peak of LiMgPO₄:Dy when calculated by using Eq. (4) was found to be $1.16 \times 10^{12} \text{ s}^{-1}$. To obtain the kinetic parameters the TL reading were carried out on powder samples at a heating rate of 5 °C /s. The low temperature peak was removed by thermal cleaning. Table 1 gives the

Table 1 Trap parameters of 160 °C glow peak of LiMgPO₄:Dy phosphor.

Trap parameters	Mean values
Symmetry factor 'μ _g '	0.43
Balarin parameter 'γ'	0.80
Order of kinetics 'b'	1
Activation energy 'E'	1.076 eV
Frequency factor 's'	$1.16 \times 10^{12} \text{ s}^{-1}$.

4. Conclusion

LiMgPO₄: Dy³⁺ phosphor was synthesized by high temperature solid-state reaction method. The PL emission spectra of LiMgPO₄:Dy³⁺ phosphor show efficient blue (483 nm) and yellow (576 nm) bands at the excitation of 350 nm wavelength of UV light. The emission spectra for the Dy³⁺ doped samples are composed of the characteristic emission lines of Dy³⁺ with ⁴f₉ configuration. The blue emission band is typical emission of Dy³⁺ ion assigned to ⁴F_{9/2} → ⁶H_{15/2} transition and yellow emission is assigned to ⁴F_{9/2} → ⁶H_{13/2} transition.

LiMgPO₄: Dy exhibits main TL peak at 160°C with a hump at 232°C. The optimum mole fraction of Dy³⁺ is 2 mol% to obtain the highest TL intensity. The TL dose-response of LiMgPO₄:Dy³⁺ to γ - ray was linear in the range of 1 to 100 Gy. TL sensitivity was observed about 1.64 times that of CaSO₄:Dy TLD phosphor. The trap parameters of the TL glow curve of the sample were calculated by the peak shape method. The activation energy and frequency factor are found to be 1.076 eV and $1.16 \times 10^{12} \text{ s}^{-1}$, respectively. The phosphor LiMgPO₄:Dy³⁺ is found to have first order kinetics in TL studies, suggesting that the probability of retrapping of charges is

negligible. The fading of the dosimetric peak is less than 10 % for 10 days if the dosimeters were protected from direct room light. The TL and dosimetric characteristics imply the potential of LiMgPO₄:Dy³⁺ phosphor as gamma-ray TL materials in the personal protection and environmental dosimetry field.

Acknowledgements

Author SPP is thankful to management of the Institution KNM, Nagpur for providing useful facilities of the instrumentation, SHIMADZU Spectrofluorophoto- meter (RF-5301 PC) to carry out this work.

REFERENCES

- [1] Lakshmanan AR, Jose MT, Ponnusamy V, Kumar P, Vivek R, Luminescence in CaSO₄: Dy phosphor - dependence on grain agglomeration, sintering temperature, sieving and washing. *J. Phys. D: Appl. Phys.* 2002; 35; 386.
- [2] Shinde SS, Dhabekar BS, Gundu Rao TK, Bhatt BC, Preparation, thermoluminescent and electron spin resonance characteristics of LiF:Mg,Cu,P phosphor. *J. Phys. D: Appl. Phys.* 2001; 34; 2683.
- [3] Salah N, Khan ZH, Habib SS, Copper

activated LiF nanorods as TLD material for high exposures of gamma-rays. *Nucl. Instrum. Meth. (B)* 2009; 267; 3562.

[4] Zahedifar M, Mehrabi M. Thermoluminescence and photoluminescence of cerium doped CaSO_4 nanosheets. *Nucl. Instrum. Meth. (B)* 2010; 268; 3517.

[5] Bangaru S, Muralidharan G. Thermoluminescence, photoluminescence, photo-stimulated luminescence and optical studies on X-ray irradiated KBr: Ce^{3+} crystals. *Nucl. Instrum. Meth. (B)* 2010; 268; 1653.

[6] Dhoble SJ, Moharil SV. Preparation and characterisation of Eu^{2+} activated $\text{Sr}_2\text{B}_5\text{O}_{10}\text{Cl}$ TLD phosphor. *J. Nucl. Instrum. Methods B* 2000; 160; 274.

[7] Menon SN, Dhabekar B, Alagu Raja E, Chougankar MP. Preparation and TSL studies in Tb activated LiMgPO_4 phosphor. *Rad. Measurements* 2012; 47; 236-240.

[8] Wanmaker WL, Spier HL. Luminescence of Copper-Activated Orthophosphates of the Type ABPO_4 ($\text{A} = \text{Ca}, \text{Sr}, \text{or Ba}$ and $\text{B} = \text{Li}, \text{Na}, \text{or K}$). *J. Electrochem. Soc.* 1962; 109; 109.

[9] Elammati L, Elouadi B, Muller-Vogt G. Study of phase transitions in the system $\text{A}^{\text{I}}\text{B}^{\text{II}}\text{PO}_4$ with $\text{A}^{\text{I}} = \text{Li}, \text{Rb}$ and $\text{B}^{\text{II}} = \text{Mg}, \text{Ca}, \text{Sr}, \text{Ba}, \text{Zn}, \text{Cd}, \text{Pb}$. *Phase Transitions* 1988; 13; 29-32.

[10] Liang CS, Eckert H, Gier TE, Stucky GD. Compositionally induced phase transitions and nonlinear optic response in ABCO_4 crystal solution phases ALiPO_4 ($\text{A} = \text{Sr}, \text{Ba}, \text{Pb}$) *J. Chem. Mater.* 1993; 5; 597-603.

[11] Dhabekar B, Menon SN, Alagu Raja E, Bakshi AK, Sinnggh AK, Chougankar MP,

Mayya YS. $\text{LiMgPO}_4\text{:Tb,B}$ – A new sensitive OSL phosphor for dosimetry. *Nucl. Instrum. Meth. Phys. Res. B* 2011; 269; 1844-48.

[12] Dwijen Singh & Dorendrajit Singh, Kinetic parameters of thermoluminescence glow curves of γ -irradiated green calcite. *Indian J Pure and Appl Phys*, 2009; 47; 409-412.

[13] Kirsh Y, Kinetic Analysis of Thermoluminescence. *Phys Stat Sol A* 1992; 129; 15-48.

[14] Rudrama Devi BH, Buddhudu S. Spectral and thermal analysis of Sm^{3+} and Dy^{3+} : B_2O_3 - BaO-LiF/AlF_3 glasses. *Indian J. Pure Appl. Phys.* 2008; 46; 825-832.

[15] Nagpure IM, Pawade VB, Dhoble SJ, Combustion synthesis of $\text{Na}_2\text{Sr}(\text{PO}_4)\text{F:Dy}^{3+}$ white light emitting phosphor. *Luminescence: Bio and Chemi.* 2010; 25; 9-13.

[16] Chen R, Glow Curves with General Order Kinetics *J. Electrochem. Soc* 1969; 116; 1254-57.

[17] Garlick GFJ, Gibson AF. The Electron Trap Mechanism of Luminescence in Sulphide and Silicate Phosphors *Proc. Phys. Soc. Lond.* 1948; 60; 574-590.

[18] Furetta C, Kitis G, Kuo CH. Kinetics parameters of CVD diamond by computerised glow-curve deconvolution (CGCD) *Nucl. Instrum. Methods Phys. Res B* 2000; 160; 65-72.

[19] Balarin M, Half width and asymmetry of glow peaks and their consistent analytical representation. *J. Therm. Anal* 1979; 17; 319-332.